Synthesis and Characterization of Praseodymium Hydroxide Nanorods by a Hydrothermal Process

Jie Zhao, Weixiang Chen,* Guiyan Yu, Xiang Li, Yifan Zheng, and Zhude Xu
Department of Chemistry, Zhejiang University, Hangzhou 310027, P. R. China

(Received February 3, 2005; CL-050152)

$Pr(OH)_3$ nanorods with 12–30 nm in diameter and 30–300 nm in length were prepared by a hydrothermal process. The as-synthesized product was characterized by XRD, TEM, and TG-DTA. The results showed that the nanorods are highly crystallized hexagonal structure and stable in the low temperature. The mechanism for the hydrothermal synthesis of $Pr(OH)_3$ nanorods was discussed.

Rare earth compounds have been widely used as high-performance luminescent devices, magnets, catalysts, and other functional materials based on the electronic, optical, and chemical characteristics resulting from their 4f electrons.[1–3] If rare earth compounds were fabricated in the form of 1D nanostructures, they would have new properties as a result of both their marked shape-specific and quantum-confinement effects. Although a number of synthetic methods have been developed to fabricate and assemble 1D nanostructures,[4–8] they often suffer from the requirements of high temperature, special conditions, tedious procedures, and catalysts or templates. Therefore, the development of practical synthesis methods of 1D nanostructures at low cost still remains a challenge.

Among the methods used in 1D nanostructure synthesis, hydrothermal process has emerged as a powerful method for the fabrication of anisotropic nanomaterials, owing to their great chemical flexibility and synthetic tunability.[9–11] Recently, Kasuga et al. treated TiO_2 in alkaline aqueous solution and obtained titanium oxide nanotubes with 100 nm in length.[12] Herein, we report a simple method for direct growth of the $Pr(OH)_3$ nanorods by facile hydrothermal treatment of the corresponding bulk crystals in the presence of alkali. The mechanism of the hydrothermal synthesis of $Pr(OH)_3$ nanorods was discussed.

A detailed description of the preparation of $Pr(OH)_3$ nanorods is as follows: All chemicals used were analytic grade reagents without further purification. 0.5 g of Pr_2O_3 was dissolved in 10% nitric acid, then 10% KOH solution was added dropwise into the above solutions to form a light green colloidal precipitates. The pH was adjusted to 12.5. The obtained suspension was transferred to a 30-mL Teflon lined stainless steel autoclave. The autoclave was sealed and maintained at 120 °C for 16 h, then cooled to room temperature. The precipitates were then filtered, washed with distilled water and ethanol to remove the ions possibly remaining in the final products and finally dried at 80 °C.

X-ray powder diffraction (XRD) patterns were recorded using a Thermo X'Tra X-ray diffractometer with Cu Kα (λ = 0.1540562 nm). Transmission electron microscope (TEM) images were taken with JEOL JEM-2010 and JEOL JEM-200CX instruments, using an accelerating voltage of 200 kV. Thermogravimetry (TG) and differential thermal analysis (DTA) (using a WCT-IA thermal system) were conducted on the powders in the 0–800 °C temperature range, with a heating rate of 10 °C/min.

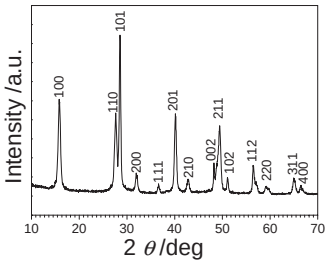

Figure 1. Powder XRD pattern of $Pr(OH)_3$ nanorods.

XRD pattern of the as-obtained $Pr(OH)_3$ product is shown in Figure 1. This indicates that the well-crystallized $Pr(OH)_3$ has major peaks at about $2\theta = 15.79°$ (100), 27.61° (110), 28.51° (101), 31.95° (200), 36.60° (111), 40.13° (201), 42.80° (210), 48.22° (002), 49.39° (211), 51.06° (102), 56.47° (220), 59.13° (310), 64.92° (311), 66.44° (400). These peaks can be perfectly indexed as a pure hexagonal phase of $Pr(OH)_3$ with calculated lattice constants $a = 6.524$ and $c = 3.785$ Å, which is consistent with JCPDS No. 45-0086. No impurity peaks can be detected in the XRD analysis; therefore, pure $Pr(OH)_3$ must have been obtained.

Figure 2 shows TEM and HRTEM micrographs and electron diffraction patterns of as-prepared $Pr(OH)_3$. From Figure 2a, it is clearly seen that $Pr(OH)_3$ precipitates are amorphous particles before the hydrothermal process. However, they become nanorods with a relatively uniform diameter ranging from 12 to 30 nm and a highly different length ranging from 30 to 300 nm (Figure 2b) after the hydrothermal treatment. The aspect ratios of these nanorods are mostly in the range of 1 to 20. This demonstrates that the as-synthesized $Pr(OH)_3$ belongs to the right kind of nanorods.[13,14] The yield of $Pr(OH)_3$ nanorods is approximately 98.3% according to repeated TEM imaging at low magnification.

Figure 2c shows the typical HRTEM image of a single $Pr(OH)_3$ nanorod. The image reveals that the lattice fringes run mainly in two different directions in the thick $Pr(OH)_3$ nanorod. One is along the direction of length of the $Pr(OH)_3$ nanorod, the other is across the direction of the length with oblique-angle. The fringes marked by the upper arrow and the lower arrow in Figure 2c are oriented along the [101] plane. The calculated interplanar distance is 0.301 nm. The orientation of the planes and their calculated interplanar distances are close to the XRD data. In addition, there are many crystal defects on the surface of $Pr(OH)_3$ nanorod. The inset of Figure 2c shows the corresponding selected area electron diffraction (SAED) pattern taken from a single $Pr(OH)_3$ nanorod, which confirmed that $Pr(OH)_3$ nanorods are hexagonal.

Figure 3 shows TG and DTA curves of as-prepared $Pr(OH)_3$ nanorods. The weight loss occurs from 320 to 360 °C. In this

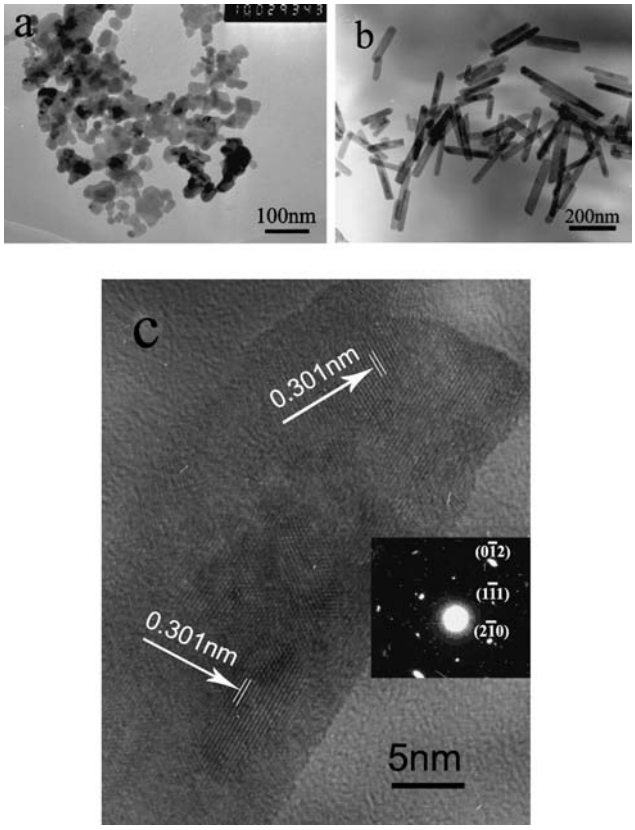

Figure 2. (a) Typical TEM image of $Pr(OH)_3$ precipitates before hydrothermal process and (b) after hydrothermal process. (c) HRTEM image of a single $Pr(OH)_3$ nanorod and the inset corresponds to its SAED pattern.

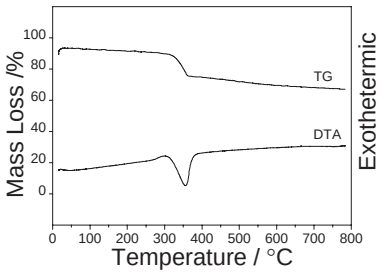

Figure 3. TG and DTA curves of $Pr(OH)_3$ nanorods.

temperature range the total weight loss was 12.7%. The weight loss in this range is due to the removal of water yielded by the decomposition of $Pr(OH)_3$ nanorods. The DTA curve exhibits endothermic peaks at 356 °C. The result demonstrates that no impurity present in the as-synthesized $Pr(OH)_3$ nanorods and they possess better stability in the low temperature.

Although the exact mechanism for the formation of these rod-like nanostructures is still unclear, we believe that the growth of the nanorods is not catalyst-assisted or template-directed. Because the source materials used in our synthesis are pure praseodymium oxide and potassium hydroxide. It is likely that the growth is governed by a solution–solid process (SS),[15] in which the oxide molecules dissolved and precipitated under the condition of alkali. The obtained praseodymium hydroxide subsequently grows into rod-like nanostructures under hydrothermal treatment. On the one hand, the morphology of the final product is largely determined by the anisotropic nature of the building block; that is, the 1D characteristics of the infinite hexagonal chains in the crystalline phase. It is reasonable to conclude that the driving force for the highly anisotropic growth of rare earth hydroxide nanorods derives from the inherent crystal structure of these materials.[16] As described above, the $Pr(OH)_3$ nanorods obtained are hexagal crystal structure, which is characteristic of highly anisotropic growth. On the other hand, in terms of hydrothermal process, KOH plays an important role as the mineralizer that dictates the nucleation and growth of nanorods. The pH of obtained suspensions was adjusted to 12.5. However, after hydrothermal process, the pH of suspension dropped to 5.2. This fact shows that the OH^- ion was concerned with the crystallization of $Pr(OH)_3$. The effect of KOH concentration on the morphology of $Pr(OH)_3$ nanorods will be further investigated in our work.

In summary, we have found a simple route to prepare ultrafine $Pr(OH)_3$ nanorods by a hydrothermal method. The $Pr(OH)_3$ nanorods were confirmed to be hexagonal, single crystalline and relatively stable in the low temperature by XRD, TEM, and TG-DTA, respectively. Such nanorods have a variety of promising applications. The simplicity of hydrothermal process, cheapness, and availability of raw materials are advantages favoring the scaling-up of nanorods.

This work was supported by the NFSC (No. 50171063) and Scientific Foundation for Returned Overseas Chinese Scholar of State Education Ministry (No. 2004-527).

References

1 G. Y. Adachi and N. Imanaka, *Chem. Rev.*, **98**, 1479 (1998).
2 A. W. Xu, Y. Gao, and H. Q. Liu, *J. Catal.*, **207**, 151 (2002).
3 A. W. Xu, Y. P. Fang, L. P. You, and H. Q. Liu, *J. Am. Chem. Soc.*, **125**, 1494 (2003).
4 M. Zhang, Y. Bando, and K. Wada, *J. Mater. Sci. Lett.*, **20**, 167 (2001).
5 L. Guo, Z. H. Wu, T. Liu, W. D. Wang, and H. S. Zhu, *Chem. Phys. Lett.*, **318**, 49 (2000).
6 X. F. Duan, J. F. Wang, and C. M. Lieber, *Appl. Phys. Lett.*, **76**, 1116 (2000).
7 A. L. Prieto, M. S. Sander, M. S. Martýín-Gonzaález, R. Gronsky, T. Dands, and A. M. Stacy, *J. Am. Chem. Soc.*, **123**, 7160 (2001).
8 A. M. Morales and C. M. Lieber, *Science*, **279**, 208 (1998).
9 Y. P. Fang, A. W. Xu, R. Q. Song, H. X. Zhang, L. P. You, J. C. Yu, and H. Q. Liu, *J. Am. Chem. Soc.*, **125**, 16025 (2003).
10 G. R. Patzke, F. Krumeich, and R. Nesper, *Angew. Chem., Int. Ed.*, **41**, 2446 (2002).
11 S. H. Yu, L. Biao, M. S. Mo, J. H. Huang, X. M. Liu, and Y. T. Qian, *Adv. Funct. Mater.*, **13**, 639 (2003).
12 T. Kasuga, M. Hiramatsu, A. Hoson, T. Sekino, and K. Niihara, *Langmuir*, **14**, 3160 (1998).
13 Y. J. Zhu and X. L. Hu, *Chem. Lett.*, **33**, 760 (2004).
14 C. J. Murphy and N. R. Jana, *Adv. Mater.*, **14**, 80 (2002).
15 J. Lu, Y. Xie, F. Xu, and L. Y. Zhu, *J. Mater. Chem.*, **12**, 2755 (2002).
16 Y. P. Fang, A. W. Xu, L. P. You, R. Q. Song, J. C. Yu, H. X. Zhang, Q. Li, and H. Q. Liu, *Adv. Funct. Mater.*, **13**, 955 (2003).

Published on the web (Advance View) April 22, 2005; DOI 10.1246/cl.2005.738